VIETNAM ACADEMY OF SCIENCE AND TECHNOLOGY

INSTITUTE OF PHYSICS

The 8th Academic Conference on Natural Science for Young Scientists Master & PhD. Students from ASEAN Countries

Vinh City, Vietnam. August 27-30, 2023

PROCEEDINGS

Publishing House for Science and Technology

VIETNAM ACADEMY OF SCIENCE AND TECHNOLOGY

INSTITUTE OF PHYSICS

THE 8th ACADEMIC CONFERENCE ON NATURAL SCIENCE FOR YOUNG SCIENTISTS, MASTER AND PhD STUDENTS FROM ASEAN COUNTRIES

(CASEAN - 8)

Vinh City, Vietnam. 27-30 August 2023

PROCEEDINGS

ISBN: 978- 604- 357- 225-4

Publishing House for Science and Technology - 2023

COMPARISON OF OPTICAL PROPERTIES OF SQUARE LATTICE PHOTONIC CRYSTAL FIBERS WITH $Ge_{20}Sb_5Se_{75}/As_2S_3$ CHALCOGENIDE GLASSES

Bao Tran Le Tran[1], Thien Nguyen Minh[1], Nam Nguyen Trong[1], Tuyet Dang Thi[1], Tan Tran Duy[2], Luu Mai Van[3], Vinh Nguyen Thanh[1], Lanh Chu Van[1*]

[1]Department of Physics, Vinh University, 182 Le Duan, Vinh City, Vietnam

[2]Truong Xuan High School, Thap Muoi District, Dong Thap Province, Vietnam

[3]Hanoi Open University, Nguyen Hien Str., Bach Khoa, Hai Ba Trung Dist., Ha Noi City, Vietnam

*E-mail: *chuvanlanh@vinhuni.edu.vn*

Abstract. In this research, we used the full-vectorial finite difference method for comparing the linear and nonlinear characteristics in the square lattice of solid-core PCFs using different substrates ($Ge_{20}Sb_5Se_{75}$ and As_2S_3). It has been demonstrated that most of the optimized As_2S_3-PCFs are superior in dispersion properties due to possessing near-zero flattened dispersion curves in the case of all-normal dispersion and anomalous dispersion with two zero-dispersion wavelengths (ZDWs). Particularly, the $Ge_{20}Sb_5Se_{75}$-PCF with one ZDW is designed to achieve an ultra-flat dispersion in the wavelength range of 5-9 μm. It is also shown that all As_2S_3 glass PCFs provide much lower confinement loss compared to fibers based on $Ge_{20}Sb_5Se_{75}$ of the same structure. The light intensity in the cores of the latter is large and hence, the nonlinear effects become more obvious. The proposed PCFs have high potential in mid-infrared supercontinuum generation.

Keywords: *Photonic Crystal Fibers, Square-lattice; Optical Characteristics; $Ge_{20}Sb_5Se_{75}$ Glass, As_2S_3 Glass.*

I. INTRODUCTION

Photonic crystal fibers (PCFs) have been a hot field of research in recent decades. PCFs have many unique features compared with conventional optical fibers such as tunable dispersion, high birefringence, high non-linearity, a maximum effective mode field area, and so on [1-10]. The advantages of these fibers consist of the control of nonlinear properties and the simplicity of dispersion engineering over the survey wavelength range. Supercontinuum spectrum (SC) generated by injecting a short input pulse with a high power to a nonlinear environment is one of their applications. It is necessary to enhance nonlinear properties and adjust of chromatic dispersion configuration of PCF for SC spectrum generation [11]. Creating an alternating cladding structure is one of these methods to accomplish it. For instance, a silica-core PCF with a triangular lattice can be designed to acquire a flat dispersion curve and a zero-dispersion wavelength (ZDW) around a wavelength of 1.55 μm [12,13]. It is interesting that PCFs with square shapes can apply the results achieved for the triangular ones. By drawing the intermediate-prepared preforms, the publication [10] demonstrated the technological feasibility of the PCFs with square lattice. For a near-zero smooth dispersion, the number of air holes has to be large, and the ratio of the air-hole size to the lattice pitch is required to be small. By a standard manufacturing process, PCFs with seven rings of air holes in the cladding have been

realized for the purpose of investigating the control and localization of high-frequency sounds [14]. Some research has been devoted to increasing the spectral bandwidth of an SC through seven-ring PCF designs with a liquid-filled hollow-core [15-17]. With small peak powers, a broad SC generation from visible to mid-infrared range can be generated in such fibers thanks to the unique advantages of the selected liquids. However, this comes at the expense of requiring a complex fluid reservoir system, and they also tend to leak outside the shell when injected into the core [18-20].

Up to now, mid-infrared PCFs have attracted great research attention from scientists around the world. On the ground of low transmission and low linearity in the infrared region, PCF made of silica is not promising for SC spectra. On the other hand, elements with good transfer and high nonlinearity in this zone are suitable, e.g., fluorite, chalcogenide, and tellurite. Among them, chalcogenide glasses offer a high linear and nonlinear refractive index, high transparency in the mid-infrared range as well a 3-10 μm light transmission range [21]. The publication [22] introduced $Ge_{20}Sb_5Se_{75}$ chalcogenide fibers for mid-infrared applications. Kai et al. analyzed the mid-infrared characterization of As_2S_3 chalcogenide glass waveguides by all-fiber structured dual-femtosecond solitons [23]. Trong et al. demonstrated the use of air-hole heterogeneity in As_2S_3 chalcogenide fibers for effective control of dispersion characteristics [24]. Therefore, $Ge_{20}Sb_5Se_{75}$ and As_2S_3 chalcogenide glasses as substrate materials are expected to be applied to design high nonlinear PCFs in the mid-infrared region.

In this paper, novel kinds of $Ge_{20}Sb_5Se_{75}/As_2S_3$ chalcogenide glasses square lattice PCF with uniform structure are proposed. A finite element method [25] combined with an optical waveguide mode theory is employed to simulate the modal properties and to study the optical properties. Finally, we compare chromatic dispersion, effective mode area, nonlinearity coefficient, and confinement loss of two above types of structures to find the most optimal PCF for SC generation.

II. PRINCIPLE OF SIMULATION

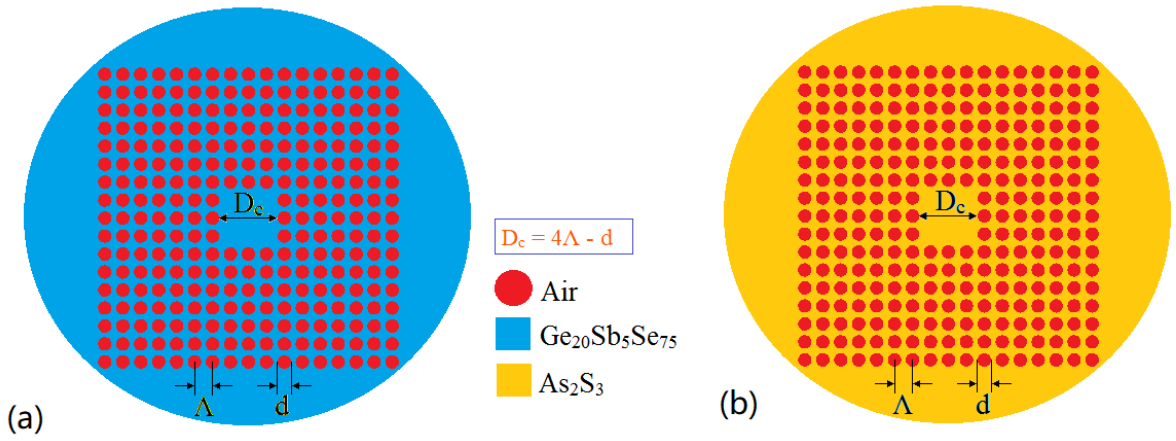

Fig. 1. *The PCF structure with chalcogenide glasses (a) $Ge_{20}Sb_5Se_{75}$ and (b) As_2S_3.*

Fig. 1 indicates the new PCF structure, in which, all circular air holes are arranged in a square lattice. The lattice pitches Λ = 1 μm, 1.5 μm, and 2 μm. d/Λ is the filling factor, equal to 0.3 – 0.7. The host materials are $Ge_{20}Sb_5Se_{75}$ (a) with nonlinear refractive index $n_{21} = 4.29\times10^{-18}$ m^2W^{-1} and As_2S_3 (b) with $n_{22} = 4.29\times10^{-18}$ m^2W^{-1}. In these structures, the core diameter (D_c)

ISBN: 978- 604- 357- 225-4

is determined as $D_c = 4\Lambda - d$ where d is the size of the air holes. The finite element method is used to calculate the linear and nonlinear optical properties of the fundamental mode at the light confinement wavelengths of each structure.

The sum of the material dispersion (D_m) and the waveguide dispersion (D_w) called chromatic dispersion (D) is calculated by [17]:

$$D = D_w + D_m \tag{1}$$

$$D_m = -\frac{\lambda}{c}\frac{\partial^2 n_m}{\partial \lambda^2} \tag{2}$$

$$D_w = -\frac{\lambda}{c}\frac{\partial^2}{\partial \lambda^2}\mathrm{Re}\left(n_{eff}\right) \tag{3}$$

where λ is the wavelength of light, n_m is the material refractive of the guided mode, and n_{eff} is the effective refractive index. n_m can be given by the Sellmeier relationships.

It can be obtained the linear refractive index of $Ge_{20}Sb_5Se_{75}$ and As_2S_3 by the Sellmeier dispersive equation [17]:

$$n^2 = 1 + \sum_{i=1}^{m}\frac{A_i\lambda^2}{\lambda^2 - B_i^2} \tag{4}$$

where $A_{11} = 4.76$, $A_{21} = 0.06$, $A_{31} = 0.89$, $B_{11} = 0.18$ μm, $B_{21} = 0.79$ μm, and $B_{31} = 22.17$ μm for $Ge_{20}Sb_5Se_{75}$ chalcogenide glass. With As_2S_3, $A_{12} = 1.89$, $A_{22} = 1.92$, $A_{32} = 0.87$, $B_{12} = 0.15$ μm, $B_{22} = 0.25$ μm, and $B_{32} = 0.35$ μm.

Confinement loss (L_c) which is one of the most important parameters in fiber transmission can be calculated [12]:

$$L_c = \frac{20}{\ln 10}\frac{2\pi}{\lambda}\mathrm{Im}\left(n_{eff}\right)\times 10^6 \tag{5}$$

III. SIMULATION RESULTS

The chromatic dispersion as a function of the wavelength is engineered by variation of the filling factor and the lattice constant. The dispersion profile for different materials is shown in Figs. 2 and 3. If the lattice constant is 1 μm, the dispersion is located in the all-normal dispersion region when $d/\Lambda < 0.4$ ($Ge_{20}Sb_5Se_{75}$) and $d/\Lambda < 0.45$ (As_2S_3). The decrease in the core diameter changes the dispersion maximum value dramatically, and the dispersion profile moves to an anomalous dispersion region. As shown in Fig. 2b, when $\Lambda = 1.5$ μm, the dispersion slopes of all structures shift toward the anomalous dispersion region with one or two zero-dispersion wavelengths (ZDW) from the normal dispersion range. The dispersion curve peak approaches shorter wavelengths with decreasing d/Λ. Further increasing in the Λ reduces the distance of neighboring ZDWs and disappears the anomalous dispersion with two ZDWs. In the case of As_2S_3, diversity of dispersion is maintained at three investigated lattice constants. As Λ increases, the number of all-normal dispersion curves becomes less, giving way to anomalous dispersion curves. It is clear that material background is another factor influencing

ISBN: 978- 604- 357- 225-4

the dispersion besides the parameters of cladding air holes. However, the fundamental mode is concentrated in the center of the fiber, hence it has little impact on dispersion.

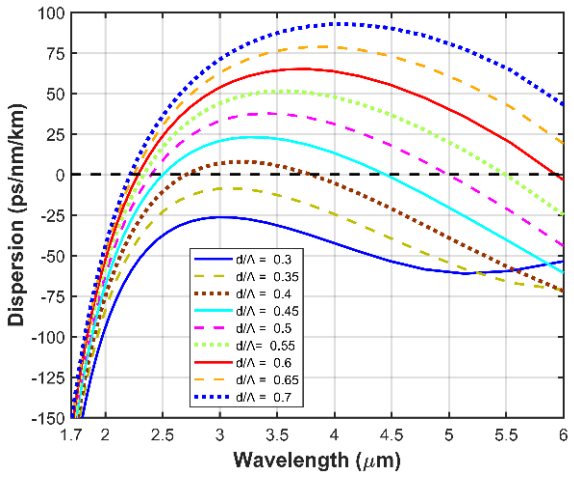

(a) Λ = 1 μm

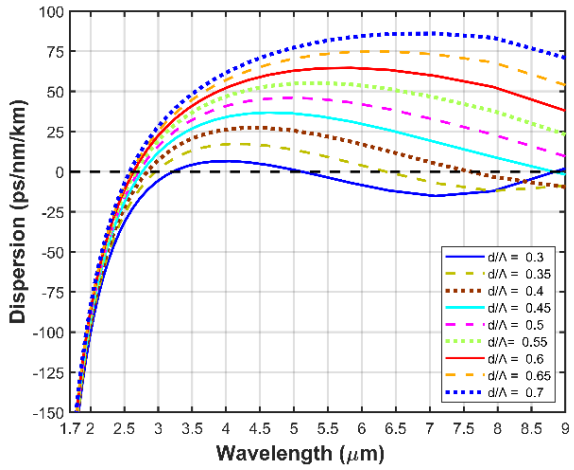

(b) Λ = 1.5 μm

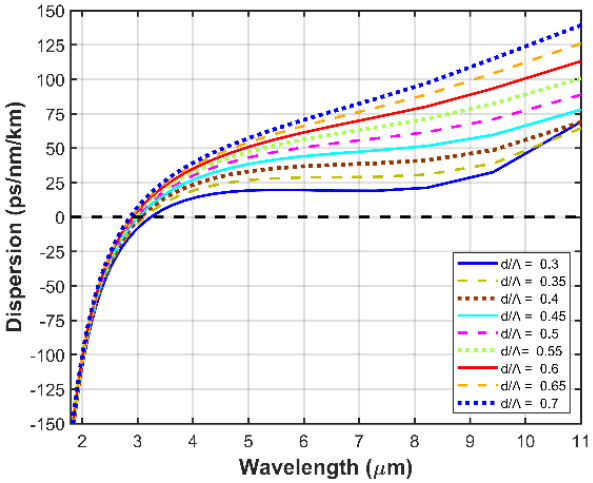

(c) Λ = 2 μm

Fig. 2. *The dispersion characteristics of $Ge_{20}Sb_5Se_{75}$ PCFs for various d/Λ and Λ.*

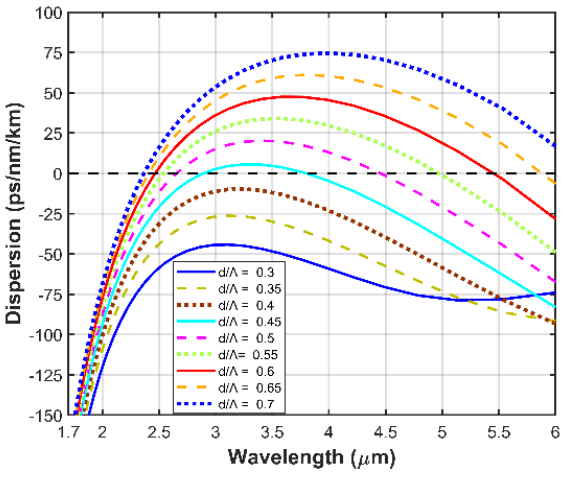

(a) Λ = 1 μm

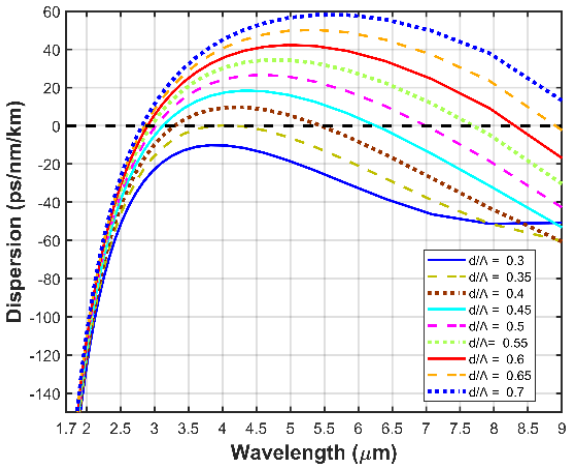

(b) Λ = 1.5 μm

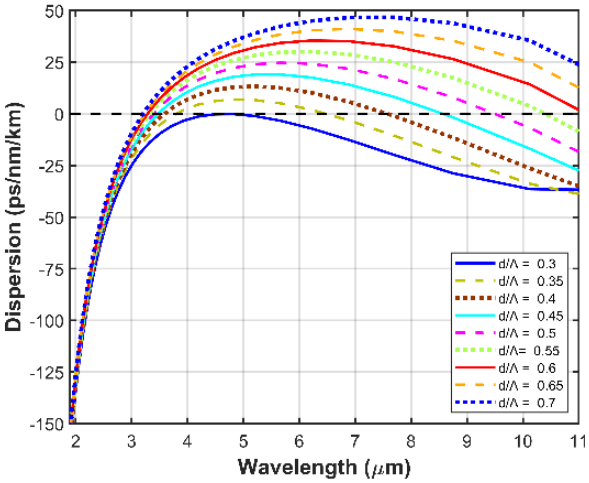

(c) Λ = 2 μm

Fig. 3. *The dispersion characteristics of As_2S_3 PCFs for various d/Λ and Λ.*

ISBN: 978- 604- 357- 225-4

In order to achieve a suitable structure for SC generation, optimal dispersion profiles are determined for different substrates. To the best of our knowledge, nonlinear effects such as Raman self-frequency shifting, dispersive wave generation, and soliton dynamics will be decisive in the process of obtaining wide SC in the anomalous dispersion regime. Whereas, the generated SC in the normal regime has the properties of a high smooth, high coherence, and pulse-preserving aspect. Therefore, for each type of material, we choose three structures corresponding to the above criteria to obtain a wide range of SC applications. Their parameters are shown in Tables 1 and 2.

Table 1. *Structural parameters of the optimized $Ge_{20}Sb_5Se_{75}$ PCFs.*

Parameters	GF_1	GF_2	GF_3
Λ	1 µm	2 µm	1.5 µm
d/Λ	0.35	0.3	0.35
D_c	3.65 µm	7.4 µm	5.475 µm

Table 2. *Structural parameters of the optimized As_2S_3 PCFs.*

Parameters	AF_1	AF_2	AF_3
Λ	2 µm	2 µm	2 µm
d/Λ	0.3	0.7	0.35
D_c	7.4 µm	6.6 µm	7.3 µm

Fig. 4a shows the presence or dispersion curves of the proposed chalcogenide PCFs. Obviously, in the all-normal and anomalous dispersion regions with two ZDWs, the optimized As_2S_3 PCFs are superior in dispersion properties because AF_1 and AF_3 possess near-zero flattened dispersion curves. If the remaining structures are considered, 4000 nm flat dispersion occurs with GF_2 which is desirable for the production of broad SC spectra.

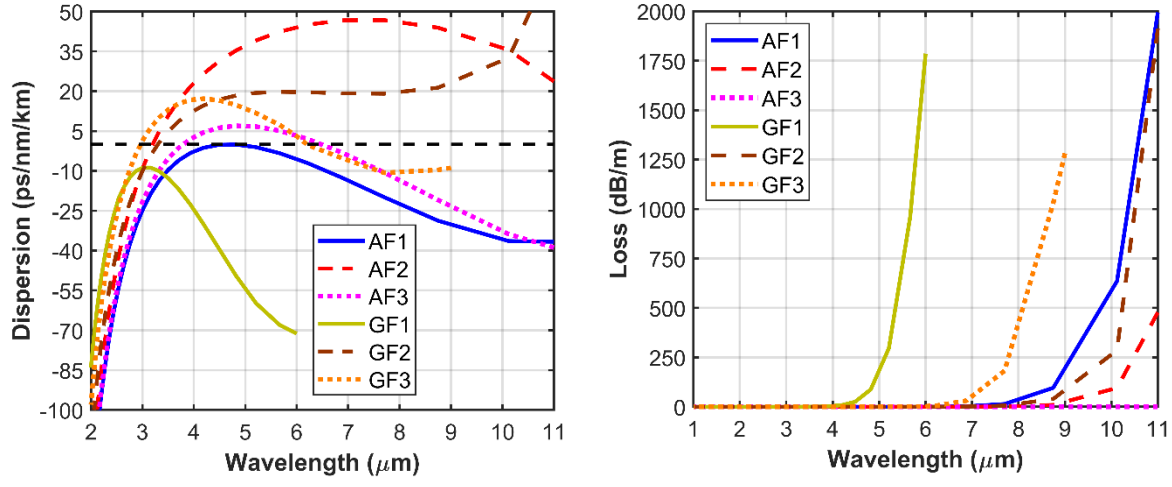

(a) (b)

Fig. 4. *The properties of proposed PCFs: (a) chromatic dispersion and (b) confinement loss.*

The change in the confinement loss characteristics for six proposed structures is shown in Fig. 4b. Generally, L_c goes up with the increase in wavelength. From this figure, it can be ascertained that most $Ge_{20}Sb_5Se_{75}$ PCFs support mode guides at shorter wavelengths than that

ISBN: 978- 604- 357- 225-4

of As_2S_3. It is found that the L_c of AF_3 is less than 10^{-14} dB/m in the 1 – 11 μm wavelength range.

Fig. 5 illustrates the efficient mode area (A_{eff}) and nonlinear coefficient (γ) of the fundamental mode for the suggested PCFs. We find that GF_1, GF_3, and AF_3 have higher nonlinear coefficients and lower effective mode areas than other fibers over the entire wavelength range.

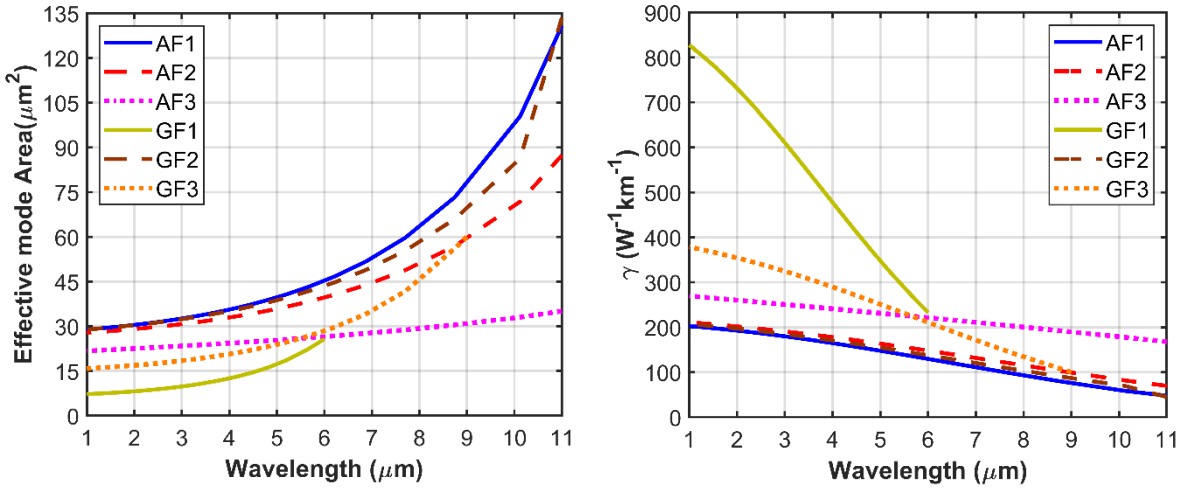

(a) (b)

Fig. 5. *The properties of proposed PCFs:*
(a) effective mode area and (b) nonlinear coefficient.

Table 3. *The characteristic values of the proposed PCFs at the pump wavelength.*

Optimal PCFs	Pump wavelength	D_c	D (ps/nm/km)	A_{eff} (μm^2)	γ ($W^{-1}km^{-1}$)	L_c (dB/m)
$Ge_{20}Sb_5Se_{75}$						
GF_1	3.25	3.65	-9.49	10.37	577.77	8.23×10^{-2}
GF_2	3.5	7.4	4.8	33.65	177.92	6.16×10^{-6}
GF_3	4.5	5.475	16.5	22.14	270.52	1.17×10^{-2}
As_2S_3						
AF_1	5	7.4	-0.54	39.6	147.58	9.21×10^{-3}
AF_2	3.5	6.6	10.67	31.77	184.47	2.05×10^{-7}
AF_3	5	7.3	6.84	25.36	231.07	7.03×10^{-15}

In Table 3, the characteristic values of the suggested PCFs at the pumped wavelength are compared with each other. It should be noted that for fibers with all-normal and anomalous dispersion with two ZDWs, the pump wavelength is chosen at the peak of the dispersion curve. Meanwhile, this value is determined at a point close to ZDW and is larger in the case of one ZDW dispersion [24]. The obtained results show that the absolute value of dispersion of AF_1 and AF_3 is smaller than that of GF_1 and GF_3. However, the latter has an advantage in effective mode area and nonlinear coefficient due to the small core sizes, especially the nonlinearity of GF_1 is nearly four times that of AF_1. On the other hand, L_c of three As_2S_3 PCFs is smaller than the others, even much lower than some previous works [12,22]. Furthermore, we also highlight

ISBN: 978- 604- 357- 225-4

their advantages due to the same air-hole diameter and the number of air-hole rings is favorable for fabrication purposes.

IV. CONCLUSION

This paper shows the optical properties of $Ge_{20}Sb_5Se_{75}$ and As_2S_3 chalcogenide glass PCFs for mid-infrared SC applications. The characteristics of these PCFs are studied by using the finite element method. When the lattice constant Λ = 1 μm, the normal and anomalous dispersions can be reached with PCFs made of $Ge_{20}Sb_5Se_{75}$ while this is present in As_2S_3 PCFs at all lattice constants considered. At wavelength λ = 5 μm, the dispersion values of AF_1 and AF_3 can reach -0.54 and 6.84 ps/nm/km, respectively, and are smaller than that of GF_1 and GF_3. Numerical results also show that the confinement loss at the pump wavelength of As_2S_3 PCFs is very small, only about 10^{-15} dB/m for AF_3. Compared to most other reports, these designs have better-confined light in the core. Here, we have obtained a small effective mode area for GF_1 and GF_3 fibers, which in turn has given us nonlinear coefficients greater than the two optimal fibers of As_2S_3. In conclusion, the proposed PCFs have a great application value for optical telecommunications, i.e., SC generation in the mid-infrared band.

ACKNOWLEDGMENTS. This research is funded by Vietnam's Ministry of Education and Training (B2023-TDV-07). Dang Van Trong was funded by the Master, PhD Scholarship Programme of Vingroup Innovation Foundation (VINIF), code [VINIF.2022.TS136].

REFERENCES

[1] J. F. Algorri, D. C. Zografopoulos, A. Tapetado, D. Poudereux and J. M. Sánchez-Pena, *Sensors*, **18**, 2018, pp. 4263.

[2] J. C. Knight, *Nature*, **424**, 2003, pp. 847.

[3] T. A. Birks, J. C. Knight and P. St. J. Russell, *Opt. Lett.*, **22**, 1997, pp. 961.

[4] R. Ahmad, M. Komanec and S. Zvanovec, *IEEE Photon. Technol. Lett.*, **28**, 2016, pp. 2736 (2016).

[5] H. Arman and S. Olyaee, *Opt. Quant. Electron.*, **52**, 2020, pp. 1.

[6] J. M. Dudley, G. Genty and S. Coen, *Rev. Modern Phys.*, **78**, 2006, pp. 1135.

[7] K. Mona, K. Arash and S. Hamed, *Optik*, **158**, 2018, pp. 142.

[8] J. C. Knight, T. A. Birks, P. St. J. Russell and D. M. Atkin, *Opt. Lett.*, **21**, 1996, pp. 1547.

[9] N. Wang, J. L. Xie, H. Z. Jia and M. M. Chen, *J. Modern Opt.*, **5**, 2018, pp. 2060.

[10] P. St. J. Russell, E. Marin, A. Díez, S. Guenneau and A. B. Movchan, *Opt. Express*, **11**, 2003, pp. 2555.

[11] L. T. B. Tran and C. V. Lanh, *Eur. Phys. J. D*, **77**, 2023, pp. 90.

[12] C. V. Lanh, N. T. Thuy, L. T. B. Tran, H. T. Duc, V. T. M. Ngoc, L. V. Hieu and H. V. Thuy, *Photonics and Nanostructures - Fundamentals and Appl.*, **48**, 2022, pp. 100986.

[13] N. N. John, K. A. Emmanuel, D. Iddrisu, D. Abert and H. Shyqyri, *Results in Opt.*, **12**, 2023, pp. 100488.

[14] R. D. S. Shreesha, T. Karpate, A. N. Ghosh, I. B. Gonzalo, M. Klimczak, and D. Pysz, R. Buczyński, C. Billet, O. Bang, J. M. Dudley and T. Sylvestre, *Opt. Lett.* **47**, 2022, pp. 2550.

[15] C. V. Lanh, H. V. Thuy, C. L. Van, K. Borzycki, D. X. Khoa, T. Q. Vu, M. Trippenbach, R. Buczyński and J. Pniewski, *Laser Phys.,* **30**, 2020, pp. 035105.

[16] B. Feroza, A. Pg. Emeroylariffion, *Prog. Electromagnetics Research C,* **89**, 2019, pp. 149.

[17] C. V. Lanh, A. Anuszkiewicz, A. Ramaniuk, R. Kasztelanic, D. X. Khoa, M. Trippenbach, and R. Buczyński, *J. Optics*, **19**, 2019, pp. 125604.

[18] A. Sharafali and K. Nithyanandan, *Appl. Phys. B,* **126**, 2020, pp. 55.

[19] L. Qiang, M. Zhuang, W. Qiang, W. Weilin, *Opt Laser Technol.,* **130**, 2020, pp. 106363.

[20] W. Chenlu, P. S. Perry, J. J. H. Dora, C. Y. Cheng, X. Zhilin, L. Shuhui, Z. Yanan, Z. Yongwei, Z. Yu, L. Baocheng, Y. Chen, T. Weijun, M. Yue and H. Georges, *OSA Continuum*, **3**, 2020, pp. 2264.

[21] W. Jiangyun, *Phys. Scr.,* **98**, 2023, pp. 055521.

[22] V. T. M. Ngoc, T. V. Thanh, C. T. H. Sam, L. T. B. Tran, D. V. Trong, N. T. Thuy, L. V. Hieu and C. V. Lanh, *Vinh Uni. J. Science*, **51**, 2022, pp. 12.

[23] X. Kai, Y. Zhen, Z. Peipei, Y. Peilong, X. Peipeng, X. Lulu, P. Xuefeng, Z. Wei, D. Shixun, W. Rongping and N. Qiuhua, *Opt. Express*, **31**, 2023, pp. 29440.

[24] D. V. Trong, L. T. B. Tran, H. T. A. Thu, N. T. Thuy and C. V. Lanh, *Vinh Uni. J. Science,* **51**, 2022, pp. 44.

[25] E. Iredia and B. I. Usiosefe, *J. Appl. Sci. Environ. Manage.*, **21**, 2017, pp. 999.

ISBN: 978- 604- 357- 225-4